OCEANS '95

MTS/IEEE

"CHALLENGES OF OUR CHANGING GLOBAL ENVIRONMENT"

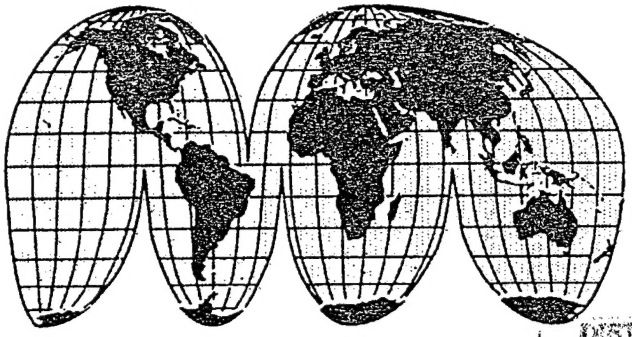

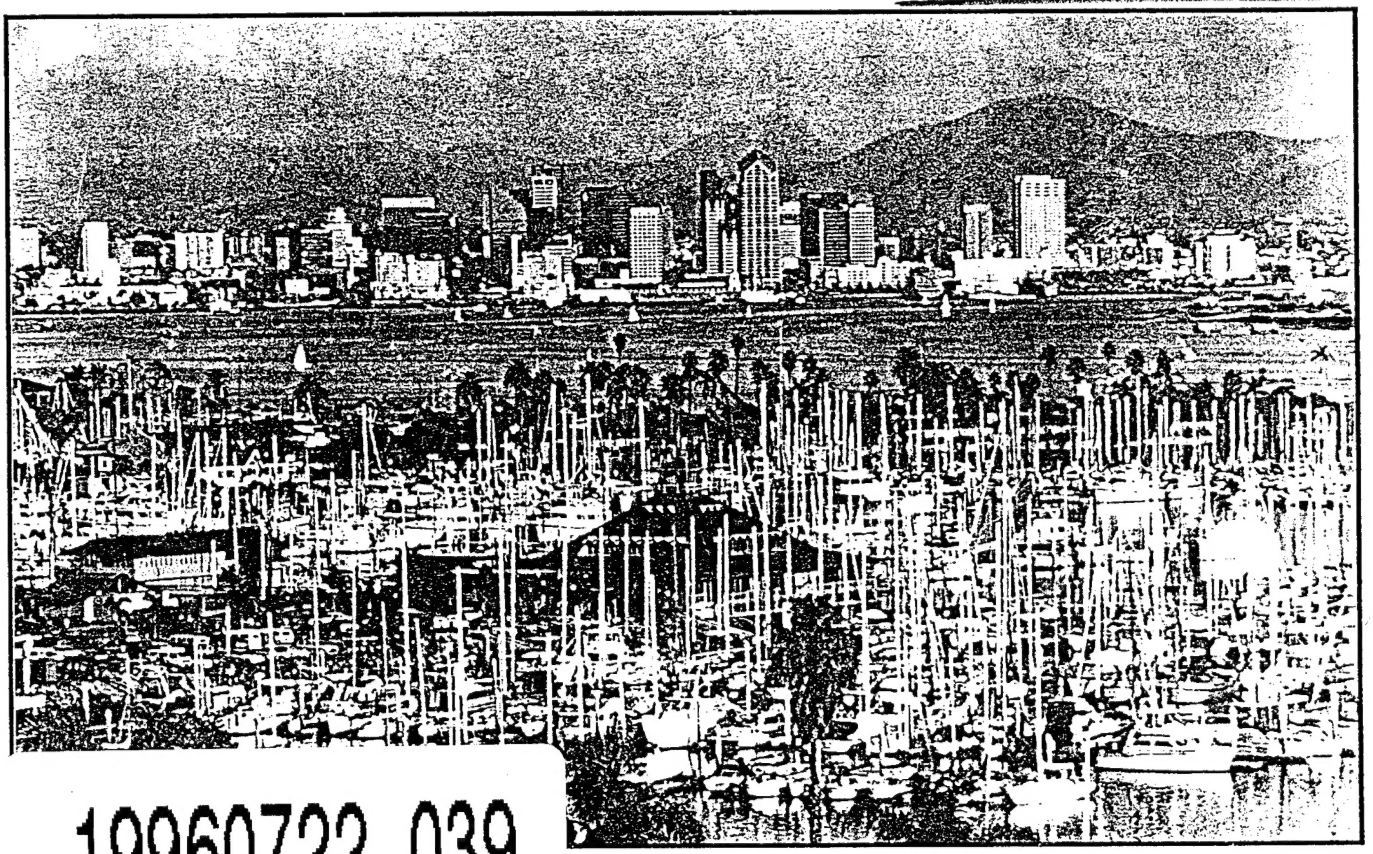

OCTOBER 9-12, 1995 • SAN DIEGO, CALIFORNIA, USA

REPORT DOCUMENTATION PAGE

Form Approved
OBM No. 0704-0188

1. AGENCY USE ONLY *(Leave blank)*	2. REPORT DATE	3. REPORT TYPE AND DATES COVERED
	October 1995	Proceedings

4. TITLE AND SUBTITLE

Sea Floor Classification by Wavelet Decomposition of Fathometer Echoes

5. FUNDING NUMBERS

Job Order No. 74513206
Program Element No. 62435N
Project No.
Task No. R035E420E0
Accession No. DN153130

6. AUTHOR(S)

[1]Russell Priebe, Nicholas P. Chotiros, [2]Donald J. Walter and Douglas N. Lambert

7. PERFORMING ORGANIZATION NAME(S) AND ADDRESS(ES)

Naval Research Laboratory
Marine Geosciences Division
Stennis Space Center, MS 39529-5004

8. PERFORMING ORGANIZATION REPORT NUMBER

NRL/PP/7431--96-0005

9. SPONSORING/MONITORING AGENCY NAME(S) AND ADDRESS(ES)

Naval Research Laboratory
Marine Geosciences Division
Stennis Space Center, MS 39529-5004

10. SPONSORING/MONITORING AGENCY REPORT NUMBER

11. SUPPLEMENTARY NOTES

Proceedings of Oceans '95 MTS/IEEE, 9-12 October 1995, San Diego, CA
[1]Applied Research Laboratories, the University of Texas at Austin, TX 78713-8029

12a. DISTRIBUTION/AVAILABILITY STATEMENT

Approved for public release; distribution unlimited.

12b. DISTRIBUTION CODE

13. ABSTRACT *(Maximum 200 words)*

Echoes reflected from the sea floor hold a great deal of information beyond what is visible in simple time series of spectra. In addition to reflections from different boundary layers, structures contained in these layers will be excited by energy from the incident pulse and may reradiate this energy. This reradiated energy will contain information about the physical nature of the structure and surrounding media. This work looks at application of time-scale signal expansions to extracting such information from fathometer echoes.

14. SUBJECT TERMS

geology, oceanography, coastal processes, mine countermeasures, and shallow water oceanography

15. NUMBER OF PAGES

9

16. PRICE CODE

17. SECURITY CLASSIFICATION OF REPORT	18. SECURITY CLASSIFICATION OF THIS PAGE	19. SECURITY CLASSIFICATION OF ABSTRACT	20. LIMITATION OF ABSTRACT
Unclassified	Unclassified	Unclassified	SAR

Sea Floor Classification by Wavelet Decomposition of Fathometer Echoes*

Russell Priebe, Nicholas P. Chotiros,
Applied Research Laboratories, the University of Texas at Austin,
Austin, TX 78713–8029 ph. 512-835-3602
Donald J. Walter, and Douglas N. Lambert
Naval Research Laboratory, Stennis Space Center, MS 39529

Abstract – *Echoes reflected from the sea floor hold a great deal of information beyond what is visible in simple time series or spectra. In addition to reflections from different boundary layers, structures contained in these layers will be excited by energy from the incident pulse and may reradiate this energy. This reradiated energy will contain information about the physical nature of the structure and surrounding media. This work looks at application of time–scale signal expansions to extracting such information from fathometer echoes.*

1 Model for Air Bubbles in Bottom Sediments

A commonly occuring sea bottom structure is constituted by gas bubbles suspended in sediment. An incident sound wave on a gas bubble surrounded by a fluid medium will excite the bubble; that is, induce oscillations in the bubble at the constituent frequencies of the sound wave. The degree of excitation of the bubble is dependent on the relationship between the spectral content of the incident wave and the natural frequencies of the system defined by the immersed bubble. Energy imparted to the bubble will be maximum at frequencies corresponding to those natural, or resonance frequencies.

If the product of the wavenumber, k_0, at the bubble's fundamental resonance and bubble radius, r, is such that $k_0 r << 1$, the immersed bubble oscillating at its fundamental resonance frequency can be modelled as a simple one degree of freedom mass–spring–damper system ([Devin 59], [Medwin 76], [Junger 86] pp. 67–69) with impulse response described by the linear second order differential equation

$$M\ddot{\zeta} + \alpha\omega M\dot{\zeta} + K\zeta = \delta(t) \tag{1}$$

Equation 1 describes the motion of the system in response to an impulse excitation $\delta(t)$, at frequency ω, with M the system mass, K the stiffness of the system, and $\alpha\omega M$ describing the energy dissipation within the system. The term α is called the system damping constant. This model assumes the energy dissipation is proportional to the bubble volume velocity, $\dot{\zeta}$. The solution to Eq. 1 is a simple exponentially damped sinusoid

$$\zeta(t) = \frac{1}{\omega_d M} e^{-\pi\alpha f t} sin(\omega_d t) u(t) \tag{2}$$

with $u(t)$ the step function, $f = \omega/2\pi$, and $\omega_d = \sqrt{1-\alpha^2/4}\omega$. Note for $\alpha << 1$, $\omega_d \approx \omega$, implying that for light damping the resonance frequency of a submerged bubble with radius r can be approximated

$$f_0 \approx \frac{\sqrt{3\gamma P_0 \rho}}{2\pi r} \tag{3}$$

Here ρ is defined as the additive density of the elements comprising the medium around the bubble, γ is the ratio of specific heats for the bubble gas, and P_0 is the static pressure in the medium. Following the development in [Devin 59], the effective system mass is due to the medium surrounding the bubble surface (this assumes that the mass of the gas inside the bubble is negligible) and is given by

$$M = \frac{\rho}{4\pi r} \tag{4}$$

The stiffness associated with the system is due to the compressibility of the gas that forms the bubble and is described by

$$K = \frac{3\gamma P_0}{4\pi r^3} \tag{5}$$

The system damping constant, α, relates the energy dissipation mechanisms at work on the system. For volume pulsations of submerged bubbles, there are three dominant mechanisms for energy dissipation. These are thermal damping due to heat conduction between the bubble gas and surrounding liquid, radiation damping as energy is transported away from the bubble acoustically, and viscous damping resulting from viscous forces at the bubble–fluid junction.

[1]This work was supported by NRL under the MTEDS program.

Detailed discussions of the damping mechanisms and expressions for α can be found in [Devin 59] and [Medwin 76]. System damping constant will be a sum of damping constants due to each of the three mechanisms cited above

$$\alpha = \alpha_t + \alpha_r + \alpha_v \tag{6}$$

where α_t, α_r, and α_v refer to damping due to thermal, radiation, and viscous mechanisms, respectively.

The significance of the bubble impulse response described in Eq. 2 is that the center frequency and decay rate are characteristic of the geometry of the bubble and the physical properties of the bubble and medium. Such information can be exploited for sediment analysis applications.

2 Wavelet Techniques

The continuous wavelet transform (CWT) is a technique which expands a signal onto a time-scale plane via correlation with a set of basis functions, called wavelets, indexed by time, b, and scale, a. Simply put, a wavelet can be any function, $h(t)$, which is bandpass and zero mean. Families of wavelets are formed by dilating, or *scaling*, and shifting $h(t)$ in time

$$h_{a,b}(t) = \frac{1}{\sqrt{a}} h\left(\frac{t-b}{a}\right). \tag{7}$$

Coefficients are generated at each point a, b in scale and time by correlating with a wavelet that has been scaled and shifted. For a signal $s(t)$ the CWT will consist of a set of coefficients, $\phi_{a,b}(s)$, generated by taking an inner product of the signal and wavelet at every point in scale and time with $\phi_{a,b}(s)$ given by

$$\phi_{a,b}(s) = \int_{-\infty}^{\infty} s(t) h^*_{a,b}(t) dt \tag{8}$$

In continuous form, the CWT is an *energy preserving transform* and will yield true time–scale energy distributions for a signal. Discrete implementations of the CWT will yield good approximations of a signals time–scale energy content if the time–scale plane is sampled densely enough [Daubechies 90]. Note also that if the spectral content of the wavelet used is unimodal with energy that is well localized in frequency there is an inverse relationship between scale and frequency. This property allows CWT's generated by such wavelets to be treated as time–frequency expansions. Because of their ability to simultaneously decompose a signal into temporal and spectral components, wavelet expansions are effective in non–stationary signal analysis.

The optimal (with respect to signal–to–noise ratio) set of basis functions on which to expand a signal are ones which precisely match the signal. However, in many cases this is not possible as the structure of a signal cannot be completely determined. Nevertheless, basis functions that closely mimic the time–scale behavior of a process can be very effective at localizing signal component energies. Wavelet transforms offer the ability to perform isometric signal expansions with a flexibility in the choice of the basis function. This flexibility can be exploited to yield processing gains and unique feature extraction capabilities.

Processes which generate transient signals in the form of exponentially damped sinusoids can be described as time–scale processes if they exhibit damping constants that are linearly proportional to frequency. This label implies that signals arising from these processes will consist of components, or modes, which possess constant time–bandwidth products. However, it is not necessary that a process be time–scale in order to be exploitable by wavelet transform techniques. The most straightforward method of tailoring a wavelet to match the signal's time–scale behavior is to use a wavelet which is a copy of the signal. In practical applications, a quadrature sampling scheme will be necessary to deal with phase differences between the sampled signals and the discrete wavelets. For processes whose components generate signals in the form of damped sinusoids, this suggests use of a damped complex exponential with added terms to give a wavelet of the form

$$e^{-(\alpha/2+j)\omega t}u(t) + t\left[je^{-t\sqrt{(\alpha^2/4+1)}\omega} - e^{-t\sqrt{2(\alpha^2/4+1)}\omega t/\alpha}\right]u(t) \tag{9}$$

Operating at ranges where $\alpha \ll 1$ and $\omega \gg 1$ will make the contributions of the last two terms in eq. 9 negligible and allow the wavelet to be approximated as

$$h_{a,b}(t) = \frac{1}{\sqrt{a}} e^{-(\alpha/2+j)\omega_\phi (t-b)/a} u(t-b) \tag{10}$$

Now note that for light damping, the impulse response of submerged gas bubbles given in Eq. 2 can be rewritten

$$\zeta(t) = Ae^{-\alpha\omega t/2} sin(\omega t)u(t)\ . \tag{11}$$

The scaling operation of the wavelet expansion described in the previous section produces basis functions in which damping is linearly proportional to frequency. This implies that wavelet expansions using damped complex exponential wavelets are optimal with respect to signal–to–noise ratio for processes producing damped sinusoidal component signals that exhibit a constant damping/frequency ratio; i.e. processes that are time–scale in nature. In the instance of bubbles suspended in fluid sediments, this requires that damping at resonance is linearly proportional to the resonance frequency. For light damping this requirement means that damping at resonance is inversely proportional to bubble radius, i.e. that α is constant. Under these circumstances, bubble radius

will be proportional to the wavelet scale variable. System damping for submerged gas bubbles is not linearly proportional to resonance frequency; however, over certain bandwidths,it may be reasonably approximated as linearly proportional to resonance frequency.

Figure 1 is the time series and power spectrum of a fathometer echo. Visible in the time series is the penetration of multiple layers on the sea floor. The spectrum indicates a broadband return. In order to examine features representative of the sea bottom it will be necessary to deconvolve the fathometer source signal from the return. Such deconvolved echoes will characterize the impulse response, or transfer function of the sea bottom. Shown in Fig. 2 is the wavelet transform of the return shown in Fig. 1 deconvolved from the source signal. This transform used the basis functions of Eq. 10 to match the bubble impulse responses described in Eq. 11. Note the numerous clusters of high energy coefficients, or *modes*, in the signal. These modes are indicative of concentrations of resonators buried throughout the bottom. Here, the resonators are gas bubbles submerged in the bottom sediment which have been excited by the incident fathometer pulse. Deconvolving the source signal yields the bubble impulse responses.

Wavelet transforms yield many important clues useful for identification and analysis of bottom sediments. Resonators such as submerged gas bubbles can be identified and localized in time (depth) and frequency. Because of the basis function used and the nature of the bubble impulse response, modal decay rates can be estimated from wavelet transform coefficients. Modal decay rates can be exploited as discriminators of the presence of submerged gas bubbles. Additionally, analysis of center frequencies and decay rates may be useful in estimating bubble sizes. Wavelet transform coefficients can also be used to estimate the energy in each mode of a signal.

For damped complex exponential wavelets applied to damped sinusoidal signals, examination of the temporal behavior of wavelet transform coefficients allows estimation of system damping, α. Assume a damped sinusoidal signal $s(t)$ which starts at time t' with amplitude A, damping constant α_s, and center frequency ω_s. It can be demonstrated that after peaking, the wavelet transform coefficients will decay at a rate that is solely a function of the signal decay rate, $\alpha_s\omega_s/2$ [Priebe 95]. For a particular mode, the decay rate can be determined by observing the temporal vector of wavelet transform coefficients containing the modal peak as it decays in magnitude beyond that peak (Fig. 3). If ϕ_{a,b_1} and ϕ_{a,b_2} are two such coefficients from that vector separated in time by $\delta t = a/(b_2 - b_1)$ then α_s can be estimated by

$$\alpha_s = \frac{2a}{\omega_\phi} \ln \frac{|\phi_{a,b_2}|}{|\phi_{a,b_1}|} \frac{a}{(b_2 - b_1)} \qquad (12)$$

Gas bubbles trapped in bottom sediments often occur in large concentrations that are excited concurrently, giving rise to coexisting multiple modes. Consider an individual signal mode with center frequency ω_s, decay rate α_s, and start time t_s which is surrounded in time and frequency by other modes with amplitudes A_n, center frequencies ω_n, decay rates α_n, and start times t_n. The energy from these nearby modes will influence the wavelet transform coefficients corresponding to the mode at ω_s, t_s. The degree of this influence will be proportional to the modal separations in time and frequency. When evaluating modal decay rates for signals with closely spaced modes (such as the signal of Fig. 2), the estimates obtained from the wavelet transform coefficients should be treated as moving averages in time and scale.

Figure 4 plots the modal damping coefficients (α) as a function of frequency for the modes of the signal of Fig. 2, a return from sediment containing submerged gas bubbles. Analysis of returns of known bubbly sediments gives a good indication of what range of modal decay rates to expect for these systems. Also on the plot of Fig. 4 is a curve showing the theoretical values for damping constant, α as a function of resonance frequency. The theoretical curve was generated based on expressions developed in [Devin 59]. It assumed constant depth air bubbles submerged in sediment whose density was twice that of water. Further, the curve also assumed spherical bubbles oscillating at their fundamental resonance frequency. Note that there is about an order of magnitude discrepancy between the theoretical curve and the mean of the measured values. This discrepancy may be due several factors, some of which are: the bubbles were generally not spherical in shape [Abegg 94] , they were distributed over a range of depths (radiation damping increases significantly with depth), the gas involved was typically methane (the curve assumed air), and the sediment density differed from the value used for the curve.

Shown in Fig. 5 are two probability density functions (pdf's) for modal decay rates. They are based on measured modal decay rates from two known bottom types – hard surface and gassy sediment. Signal modes connected with reflection at interfaces will exhibit higher decay rates which tend to be more characteristic of the source transfer function (as evidenced by the pdf corresponding to the hard surface data). Decay rates from the gassy sediments tended to be more lightly damped. Note that the pdf's did not distinguish modal sources within the individual echoes. All modes present within a ping were used to generate the pdf for that particular bottom type. Hence, more highly damped modes resulting from reflection at interfaces are included in the pdf for gassy sediment.

Figure 5 was used to implement a simple bottom classification scheme. By analyzing fathometer echoes from a ship moving at about 4 knots and sounding once a second a bottom map of a section of Eckernfoerde Bay was generated. This map is displayed in Fig. 6. The map was formed by averaging modal decay rates

from deconvolved fathometer echoes over cells of 0.1 meter resolution in depth within each echo. Any cells with three or more modes present whose average decay rate fell between 0.005 and 0.0328 were classified as gassy sediments and are shown as gray areas on the map. Cells with three or more modes present whose average decay rate exceeded 0.0328 were classified as interfaces. These are the white areas on the map.

Other useful features can be extracted from fathometer echo wavelet transforms. These include modal density (simply the number of modes in an echo) and penetration (defined as the maximum range difference between modes in an echo). Pdf's for each of these features are shown in Figures 7 and 8 for echoes from hard surfaces and gassy sediments. While modal density and penetration may not be unique to any particular bottom class, using these two features along with modal decay rates may provide useful sea floor classification tools.

3 Conclusions

The wavelet transform offers a practical tool for echo sounder signal analysis because of its ability to decompose these signals into their constituent modes and extract relevant features from those modes. By examining the modal features, judgments can be made as to the nature of any underlying structure in the sea floor. These methods have been demonstrated to be particularly suited to detecting submerged gas bubbles. Further, use of multiple features available from echo–sounder signal decomposition has potential for wider applications to sea floor classification.

References

[Junger 86] Junger,M., and Feit,D. *Sound, Structures, and Their Interaction*,MIT Press, Cambridge, 1986

[Devin 59] Devin, C."Survey of Thermal, Radiation, and Viscous Damping of Pulsating Air Bubbles in Water", *Journal of the Acoustical Society of America*, **31** (12), Dec. 1959, pp. 1654-1667

[Medwin 76] Medwin, H. "Counting bubbles acoustically: a review", *Ultrasonics*, Jan. 1977, pp. 7-13

[Daubechies 90] Daubechies, I. (1990). "The Wavelet Transform, Time-Frequency Localization and Signal Analysis," *IEEE Transactions on Information Theory*, Vol. 36, No. 5, pp. 96-1005, Sept. 1990

[Priebe 95] Priebe, R. (1995) *Wavelet Applications to Detection and Classification of Impulsive Metallic Transients*, Ph.D. Dissertation, University of Texas at Austin

[Abegg 94] Abegg, F., Anderson, A., Buzi, L., Lyons, A., and Orsi, T. (1994) "Free Methane Concentration and Bubble Characteristics in Eckernforde Bay, Germany", in *Proceedings of the Gassy Mud Workshop held at the FWG, Kiel, 11-12 July 1994*, Thomas Wever, editor, Kiel, Dec. 1994

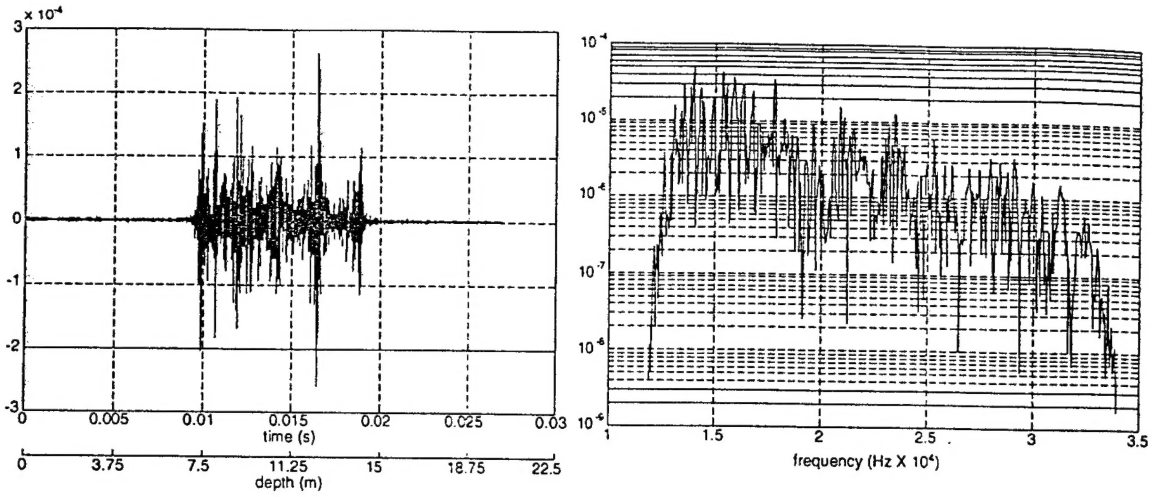

Figure 1: *Fathometer echo from gassy sediment.*

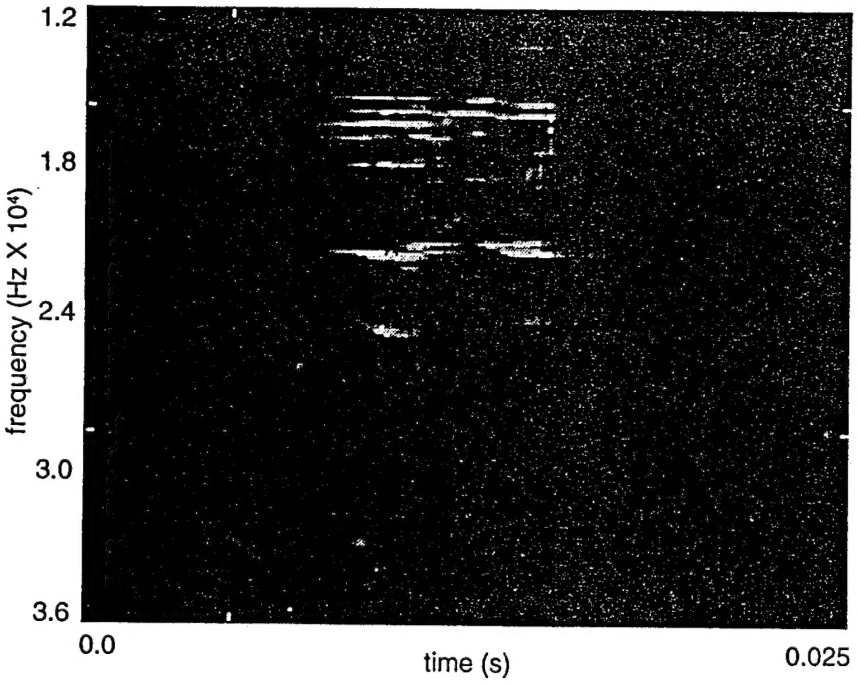

Figure 2: *Wavelet transform of fathometer echo of Figure 1. Coefficient energy levels are mapped to colors. Signal modes are clearly visible.*

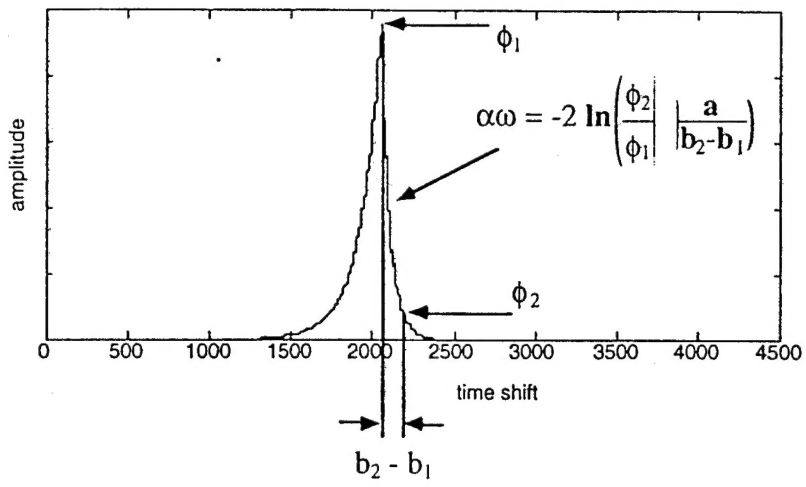

Figure 3: *Estimation of modal decay rate of a damped sinusoidal signals by examination of the temporal vector of wavelet transform coefficients containing the modal peak. This technique assumes use of a damped complex exponential wavelet.*

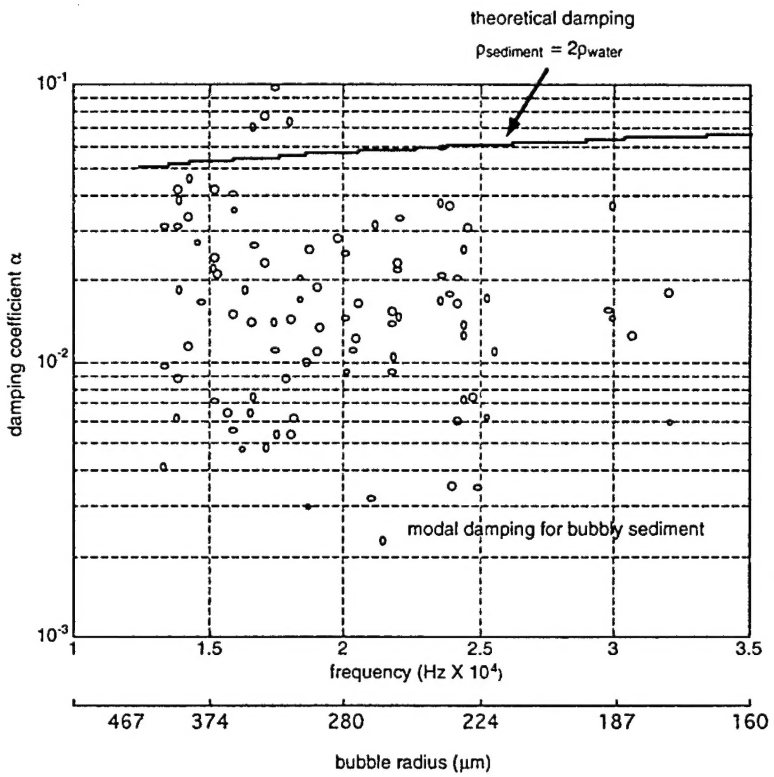

Figure 4: *Plot of damping constants for signal modes of impulse response shown in Figure 2 vs. bubble resonance frequencies. Overlaid on the plot is a curve showing theoretical damping constants for air bubbles in sediment at 20m depth for band of interest. Below the frequency scale is a scale showing the bubble radius associated with the resonant frequencies of the theoretical curve.*

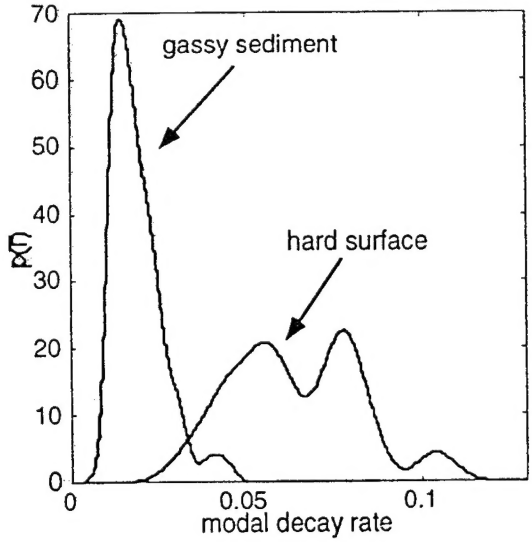

Figure 5: *Probability density functions for modal decay rates evident in echoes from known hard surfaces and gassy sediments.*

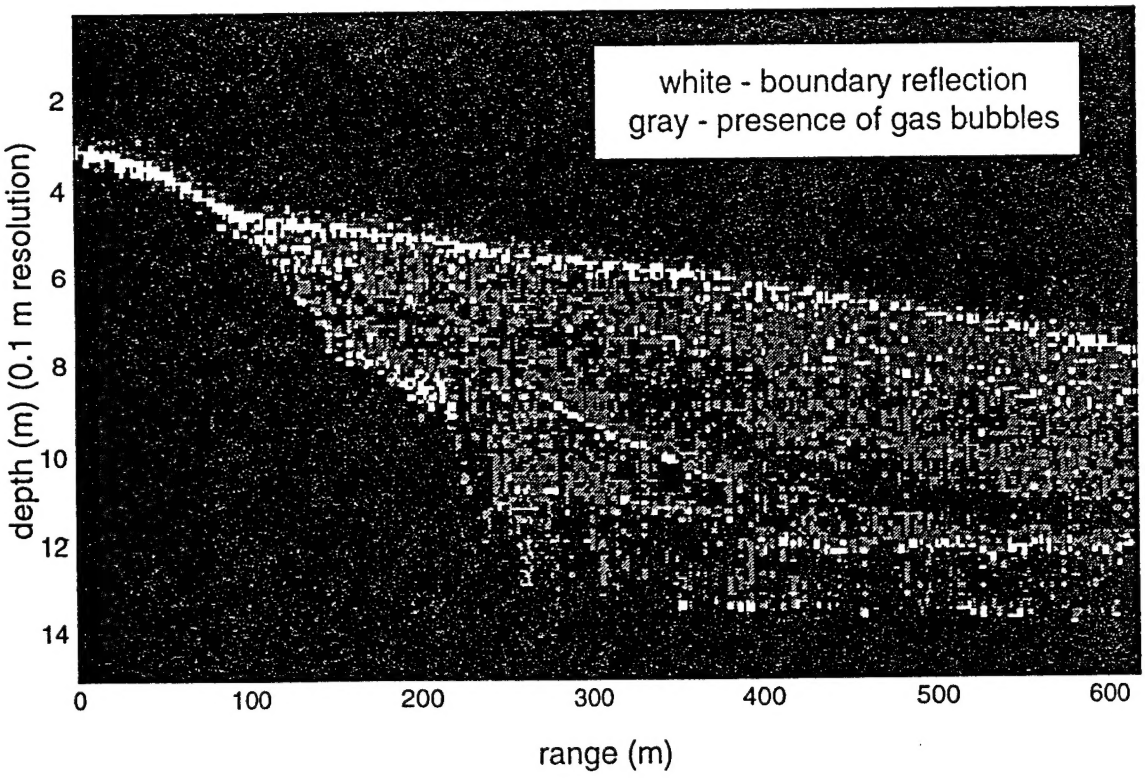

Figure 6: *Sea floor classification map of modal decay rates for section of Eckernfoerde Bay.*

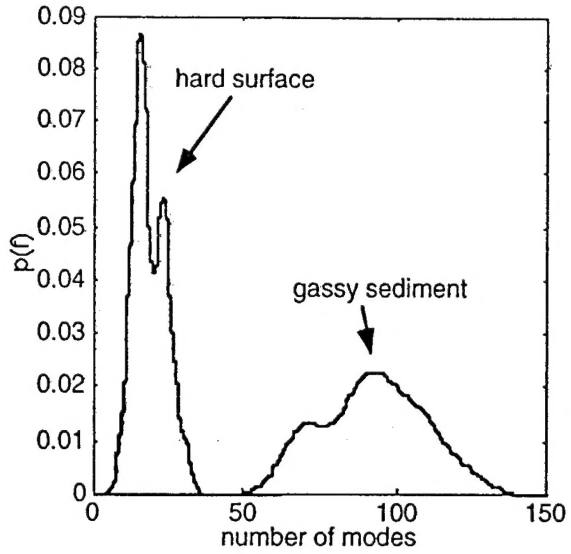

Figure 7: *Probability density functions for modal densities evident in fathometer echoes from known hard surfaces and gassy sediments.*

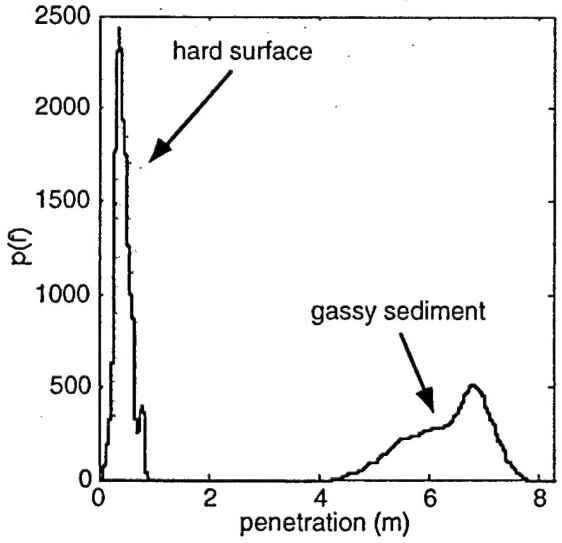

Figure 8: *Probability density functions for penetration evident in fathometer echoes from known hard surfaces and gassy sediments.*